

Corrosion study of pipeline carbon steel in sour brine under turbulent flow conditions at 60°C

R. Galvan-Martinez^{1*}, R. Orozco-Cruz¹, G. Galicia-Aguilar¹, A. Contreras²
J. Mendoza-Flores², J. Genesca-Llongueras³

¹Unidad Anticorrosión, Instituto de Ingeniería, Universidad Veracruzana, Av. S.S. Juan Pablo II s/n, Zona Universitaria, Veracruz, México. ²Instituto Mexicano del Petróleo, Eje Central L. Cárdenas Norte 152, San Bartolo Atepehuacan, México. ³Universidad Nacional Autónoma de México, Facultad de Química, Departamento de Metalurgia, Ciudad Universitaria, México.

Estudio de la corrosión de un acero al carbono de tubería en salmuera amarga bajo condiciones de flujo turbulento a 60°C

Estudi de la corrosió d'un acer al carboni de canonada en salmorra amarga en condicions de flux turbulent a 60°C

Recibido: 10 de diciembre de 2012; aceptado: 11 de febrero de 2013

RESUMEN

El presente trabajo exhibe los resultados electroquímicos obtenidos durante el estudio de la corrosión de una muestra de tubería de acero X52 inmersa en una solución "amarga" bajo condiciones de flujo turbulento a 60°C. Para obtener la información de la cinética del acero, se utilizaron las técnicas de curvas de polarización, impedancia, resistencia a la polarización lineal y el método de pérdida de peso a diferentes tiempos de inmersión. Se utilizó un electrodo cilíndrico rotatorio para controlar las condiciones de flujo turbulento y las velocidades de rotación fueron: condiciones estáticas (0 rpm) y de flujo turbulento (1000 rpm). Se realizó un análisis superficial para determinar la morfología del proceso de corrosión y las fases que constituyen los productos de corrosión. En general, se encontró que el flujo tiene una considerable influencia sobre los procesos electroquímicos que ocurren en la superficie del acero. Además, la velocidad de corrosión aumentó a medida que la velocidad de flujo también aumentó. En el análisis superficial se encontraron tres fases, mackinawita (Fe,Ni)_{1+x}S, pirrotita (Fe_(1-x)S) y marcasita (FeS₂). Un ataque localizado fue encontrado en las dos salmueras bajo ambas condiciones.

Palabras clave: Flujo turbulento, impedancia, electrodo cilíndrico rotatorio, acero X52, H₂S.

SUMMARY

This work presents the electrochemical results obtained during the corrosion study of X52 pipeline steel sample, immersed in "sour" solution under turbulent flow conditions at 60°C. In order to obtain information on the corrosion kinetics, weight loss method, linear polarization resistance, impedance and polarization curves were used at different immersion times. In order to control the turbulent flow conditions, a rotating cylinder electrode was used at two different rotation rates, 0 and 1000 rpm. A surface analysis was carried out in order to identify the corrosion

morphology and the corrosion product formed on the steel sample. In general, it was found that flow has a considerable influence upon the electrochemical process occurring on the surface of the steel. It was observed as the flow rate increased the corrosion rate also increased. In surface analysis three phases were found, mackinawite (Fe,Ni)_{1+x}S, pyrrhothite (Fe_(1-x)S) and marcasite (FeS₂). In addition, a "localized attack" was found.

Keywords: Turbulent flow, impedance, rotating cylinder electrode, X52 steel, H₂S.

RESUM

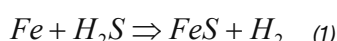
Aquest treball mostra els resultats electroquímics obtinguts durant l'estudi de la corrosió d'una mostra de canonada d'acer X52 immersa en una solució "amarga" en condicions de flux turbulent a 60 °C. Per obtenir la informació de la cinètica de l'acer, es van utilitzar les tècniques de corbes de polarització, impedància, resistència a la polarització lineal i el mètode de pèrdua de pes a diferents temps d'immersió. Es va utilitzar un elèctrode cilíndric rotatori per controlar les condicions de flux turbulent i les velocitats de rotació van ser: condicions estàtiques (0 rpm) i de flux turbulent (1000 rpm). Es va realitzar una anàlisi superficial per determinar la morfologia del procés de corrosió i les fases que constitueixen els productes de corrosió. En general, es va trobar que el flux té una considerable influència sobre els processos electroquímics que ocorren a la superfície de l'acer. A més, la velocitat de corrosió va augmentar a mesura que la velocitat de flux també augmentava. En l'anàlisi superficial es van trobar tres fases, mackinawita (Fe, Ni)_{1+x}S, pirrotita (Fe_(1-x)S) i marcassita (FeS₂). Es va detectar un atac localitzat en les dues salmorres en ambdues condicions.

Paraules clau: Flux turbulent, impedància, elèctrode cilíndric rotatori, acer X52, H₂S.

*Corresponding author: rigalvan@uv.mx

INTRODUCTION

The "sour solution" (aqueous solution containing dissolved hydrogen sulphide) can produce failures in the structures and pipelines steel in the oil and chemical industry. Most of the works and studies aimed to provide technical solutions to hydrogen sulphide (H_2S) corrosion, for example, the development of new more resistant metallic and non-metallic materials, development of organic inhibitors, studies aimed to the understanding of the combined effect of mechanical stresses and corrosion, etc.¹⁻³ The H_2S has been associated to damages by corrosion and stress corrosion cracking induced by sulphides or hydrogen.⁴⁻⁶ The increment of temperature and/or pressure can increase the aggressiveness of H_2S solution to carbon steel. Corrosion of steel in H_2S containing solutions can be represented according to⁷⁻⁹:



The majority of studies on the corrosion of steels in environments containing dissolved H_2S , have been carried out under static conditions.^{10,11} The most common type of flow conditions found in industrial processes is turbulent; however, few corrosion studies in controlled turbulent flow conditions are available. With the increasing necessity to describe the corrosion of metals in turbulent flow conditions some laboratory hydrodynamic systems have been used with different degrees of success.^{12,13} Among these hydrodynamic systems, rotating cylinder electrodes (RCE), pipe segments, concentric pipe segments, submerged impinging jets and close-circuit loops have been used and have been important in the improvement of the understanding of the corrosion process taking place in turbulent flow conditions.¹⁴⁻¹⁶

The use of the RCE, as a laboratory hydrodynamic test system, has been gaining popularity in corrosion studies.¹⁷⁻¹⁹ This popularity is due to its characteristics, such as, its operation mainly in turbulent flow conditions, its well-defined hydrodynamics, ease of assembly and disassembly, smaller volume of fluid used, and easier flow and temperature control.²⁰⁻²³ The RCE in corrosion laboratory studies is a useful tool for the understanding of mass transfer processes, effects of surface films, inhibition phenomena, etc., taking place in turbulent flow conditions.^{24,25}

EXPERIMENTAL PROCEDURE

Test environment

All experiments were carried out at 60°C and at the atmospheric pressure of Mexico City (0.7 bar). Two aqueous solutions were used: NACE brine specification 1D196 (see table 1) and a 3.5% sodium chloride (NaCl) aqueous solution. These test environments were selected due to the fact that most of the H_2S corrosion laboratory testing is carried out in this solution. In order to remove oxygen from the test environment, N_2 gas was bubbled into the test solution for a period of 30 minutes. The measured dissolved O_2 content was lower to 10 ppb. After oxygen removal, H_2S was bubbled into the test solution until saturation was reached. The measured saturation pH was 4.4 for the NACE brine solution and 4.5 for 3.5% NaCl brine. In order to determine the purging time needed to remove all O_2 from the solution, a rotating cylindrical platinum electrode was cathodically

polarized in a 1 M sodium sulphate solution, at room temperature and at different rotation rates. It was established that the region associated to the mass transfer reduction of oxygen, on the cathodic polarization curve, disappeared after 30 minutes of purging time.

Table 1. NACE brine composition. The composition is per 19 litres of distilled water.

| CHEMICAL REAGENT | Weigh (g) |
|-------------------------------|-----------|
| Calcium chloride dihydrate | 85.07 |
| Magnesium chloride sixhydrate | 39.16 |
| sodium chloride | 2,025 |

Experimental set-up

An air-tight three-electrode electrochemical glass cell was used. Cylindrical working electrodes made of API X52 pipeline steel, were used in all experiments. The total exposed area of the working electrodes was 5.68 cm² for static conditions and 3.4 cm² for turbulent flow conditions. Prior to each experiment the steel working electrodes were polished up to 600 grit SiC paper, cleaned and degreased with acetone. As reference electrode a saturated calomel electrode (SCE) was used. In order to minimize the effect of the solution resistance a Lugging capillary was used. A sintered graphite rod was used as auxiliary electrode. Hydrodynamic conditions were controlled using a RCE system. In turbulent flow condition, a rotation speed of 1000 rpm was used.

Electrochemical tests

In order to get the electrochemical measurements, linear polarisation resistance (LPR) and electrochemical impedance spectroscopy (EIS) were carried out at several time intervals, during a 24 hours period. Polarisation curves were also obtained in this study. All electrochemical tests were carried out on clean samples and in freshly prepared test solutions. In potentiodynamic LPR method a potential range of ± 0.015 V referred to E_{corr} was selected, the sweep rate was 0.001V s⁻¹. In all EIS tests, the frequency range used was 0.01 Hz to 10 kHz with a ± 0.01 V of amplitude and 5 points per decade of frequency were recorded. Potentiodynamic polarisation curves were recorded at a sweep rate of 0.001 V s⁻¹. The weight loss method was performed in order to get of corrosion rate. In this case, the working electrode was exposed in the solution for 5 days. After experimentation, selected samples were cleaned and analysed in a scanning electron microscope (SEM) and the corrosion products were analysed by X-ray diffraction (XRD).

RESULTS AND DISCUSSION

Corrosion potential vs. time

Fig. 1 shows the variation of the measured corrosion potential (E_{corr}) with time in the NACE and 3.5% NaCl solutions saturated with H_2S . In this figure is possible to see that the E_{corr} values for 3.5% NaCl solution at static conditions are more electronegative than E_{corr} values corresponding to NACE brine. At turbulent flow condition (1000 rpm), the E_{corr} values in the first 18 hours, show that the solution compositions do not have influence on the E_{corr} measured. In general, the E_{corr} values are similar in both solutions. It is important to mention that as the exposure time increased,

the E_{corr} values at static conditions have a stable increment during experiment, but on the other hand, at turbulent flow conditions, the E_{corr} values increase and diminish throughout experiment.

Linear polarisation resistance (LPR)

Fig. 2 shows the variation with time of the corrosion rate (CR) values obtained in the LPR tests. It is clear that flow affects the measured CR. In both NACE and 3.5% NaCl solutions, CR increased as the rotation of the RCE is increased. At static condition and at the beginning of the experimentation, all measured CR moves to higher values and as the exposure time increased, these are changing to stable values. This behaviour can be attributed to the fact that at the beginning of the experimentation, the surface of the steel was clean and consequently active. After a period of time, a corrosion products film formed on the surface of the working electrode, isolating the metal from the environment and decreasing CR. According some researchers, the first product of the corrosion film formed on surface of the steel in "sour" environment is mainly mackinawite.^{12,26,27}

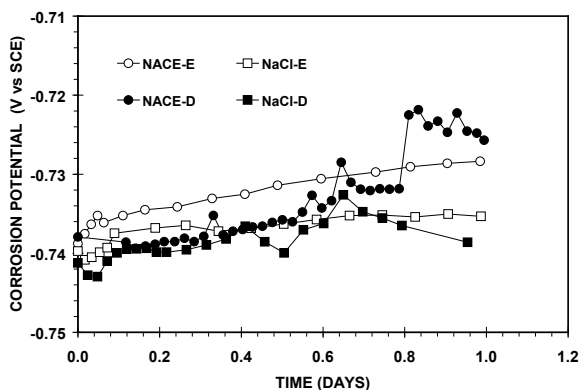


Fig. 1. Measured E_{corr} of X52 steel in NACE and 3.5% NaCl solutions saturated with H_2S at static (hollow markers, -S) and turbulent flow (filled markers, -D) conditions.

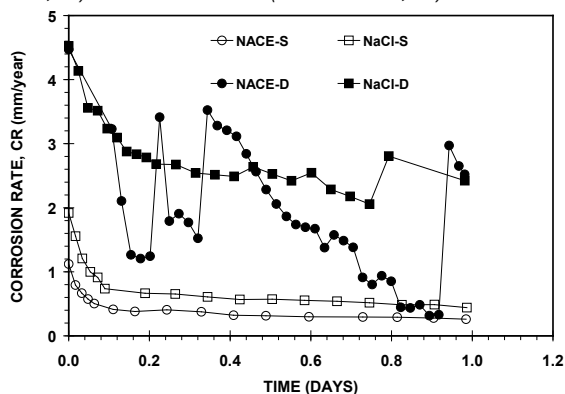


Fig. 2. CR calculated by LPR technique, as a function of time. X52 steel in NACE and 3.5% NaCl solutions saturated with H_2S at static (hollow markers, -S) and turbulent flow (filled markers, -D) conditions and 60°C.

At turbulent flow condition, the behaviour of the corrosion phenomenon at the beginning of the experimentation is similar to static condition, but as the exposure time increased, the CR values increased and diminished throughout experiment. This fact can be attributed that when the corrosion products film is broken, the measured CR increases and then, when the corrosion products film is recove-

red, the CR diminish. In addition, in both conditions, static and turbulent flow, the highest CR was measured in the 3.5% NaCl solution.

Electrochemical Impedance Spectroscopy (EIS)

Fig. 3 to 6 show the impedance spectra taken on a X52 pipeline steel immersed in NACE and 3.5% NaCl solutions saturated with H_2S , under static (Fig. 3 and 4) and turbulent flow (Fig. 5 and 6) conditions at 60°C. These figures show the impedance data obtained at five selected exposure times.

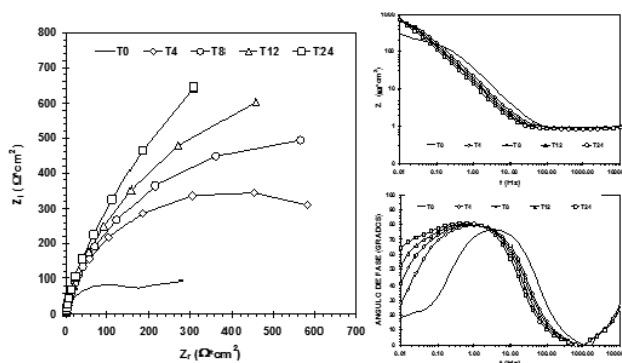


Fig. 3. Measured EIS spectra (Nyquist and Bode plots) as a function of time. X52 steel in NACE brine saturated with H_2S , static condition and 60°C. T0, T4, T8, T12 and T24 corresponding to 0, 4, 8, 12 and 24 hours of time exposition.

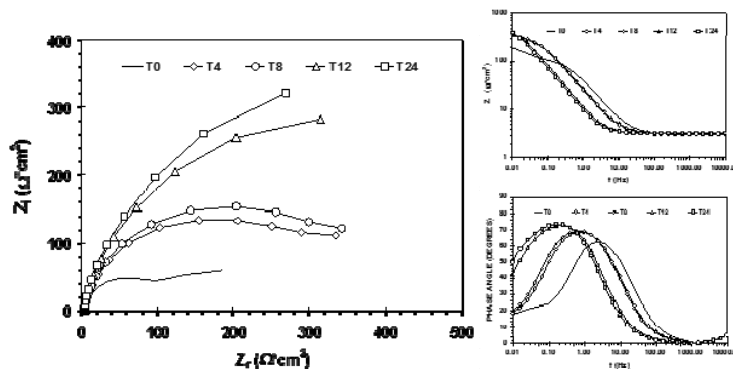


Fig. 4. Measured EIS spectra (Nyquist and Bode plots) as a function of time. X52 steel in 3.5% NaCl solution saturated with H_2S , static condition and 60°C. T0, T4, T8, T12 and T24 corresponding to 0, 4, 8, 12 and 24 hours of time exposition.

Fig. 3 and 4 shows that at the beginning of the experimentation (T0) is possible to see a second incomplete semicircle, so these Nyquist plots show two time constants corresponding to two different processes. Where, the incomplete semicircle formed at low frequencies correspond to resistance of the charge transfer process and the semicircle located at high frequencies correspond to resistance of the corrosion products film formed on surface of the X52 steel.

In the next four exposure time, the impedance spectra show that these two semicircle or time constants become one (representing one process) characteristic of the charge transfer process. In general, when the exposure time incremented, the semicircle diameter corresponding to charge transfer process increased. Bodes plot in Fig. 3 and 4 shows that the impedance spectra moved to low frequencies, in addition, a second time constant is possible

to see in the impedance spectrum at the beginning of the experimentation.

Fig. 5 and 6 show the impedance spectra taken on a X52 pipeline steel immersed in NACE and 3.5% NaCl solutions saturated with H₂S at turbulent flow conditions and 60°C. The impedance spectra show that as the exposure time increased the real impedance (Z_r) moved to highest values of resistance, except Z_r corresponding to NACE brine at 24 hrs, it is diminished. These figures also show in both test solution, that the variation in the diameter of the spectra impedance is small, 20 ohms approximately. This fact is attributed to that measured impedance values were made under turbulent flow condition. Bodes plot in these figures are agree with Nyquist plot.

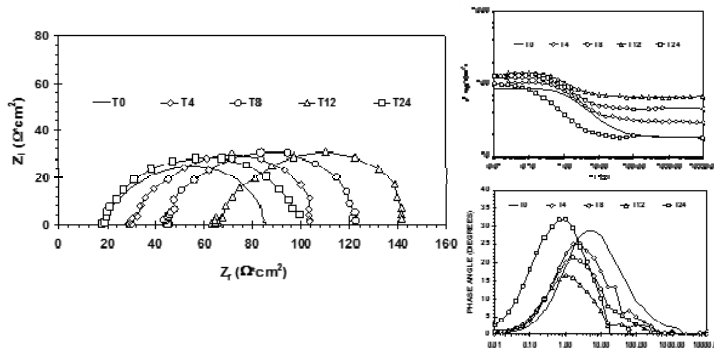


Fig. 5. Measured EIS spectra (Nyquist and Bode plots) as a function of time. X52 steel NACE brine saturated with H₂S, turbulent flow condition and 60°C. T0, T4, T8, T12 and T24 corresponding at 0, 4, 8, 12 and 24 hours of time exposition.

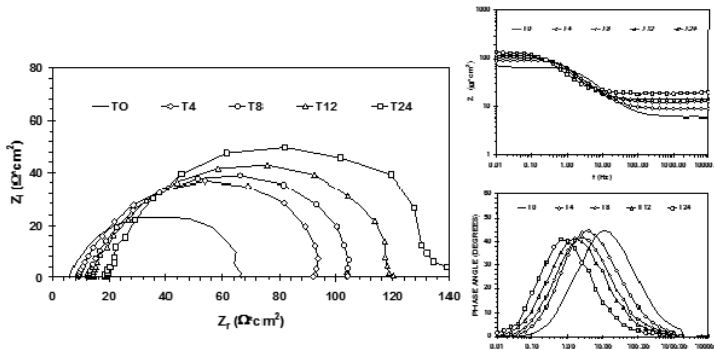


Fig. 6. Measured EIS spectra (Nyquist and Bode plots) as a function of time. X52 steel 3.5% NaCl solution saturated with H₂S, turbulent flow condition and 60°C. T0, T4, T8, T12 and T24 corresponding at 0, 4, 8, 12 and 24 hours of time exposition

Impedance spectra analysis using equivalent circuits

Fig. 7a (static conditions) and 7b (turbulent flow conditions) show the two electrical equivalent circuits used in this work for the analysis of EIS data.

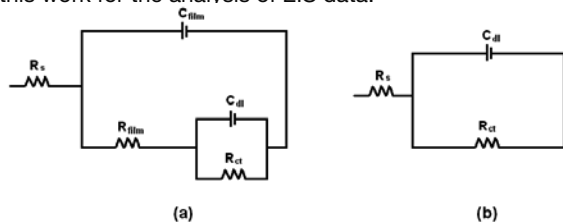


Fig. 7. Proposed equivalent circuits for static (a) and turbulent flow (b) conditions

Table 2. Resistances obtained in the equivalent circuit analysis (Fig. 7a) corresponding to impedance spectra of the corrosion of the X52 pipeline steel immersed in NACE brine saturated with H₂S at static conditions and 60°C.

| Time (h) | R _s (Ω.cm ²) | R _{ct} (Ω.cm ²) | R _{film} (Ω.cm ²) | i _{corr, Rct} (A/cm ²) | CR _{Rct} (mm/year) |
|---------------------------|-------------------------------------|--------------------------------------|--|---|-----------------------------|
| NACE Brine | | | | | |
| 0 (T0) | 0.88 | 136.49 | 181.76 | 1.90E-04 | 2.21 |
| 4 (T4) | 0.95 | 567.09 | 144.22 | 4.58E-05 | 0.53 |
| 8 (T8) | 0.87 | 781.00 | 170.12 | 3.33E-05 | 0.39 |
| 12 (T12) | 0.88 | 1025.81 | 215.67 | 2.53E-05 | 0.29 |
| 24 (T24) | 0.87 | 1450.67 | 239.41 | 1.79E-05 | 0.21 |
| 3.5% NaCl Solution | | | | | |
| 0 (T0) | 1.38 | 87.47 | 84.46 | 2.97E-04 | 3.45 |
| 4 (T4) | 0.97 | 269.74 | 191.3 | 9.64E-05 | 1.12 |
| 8 (T8) | 0.97 | 334.72 | 213.97 | 7.77E-05 | 0.90 |
| 12 (T12) | 0.98 | 382.55 | 215.78 | 6.80E-05 | 0.79 |
| 24 (T24) | 0.97 | 415.09 | 262.76 | 6.26E-05 | 0.73 |

Table 2 shows the best fitting parameters of resistances obtained in the numerical simulation of the corrosion phenomenon at static conditions, for the two test solutions and at different exposure times. In this table it can be seen that the R_{ct} and the R_{film} increased (in both test solutions) with time, consequently the calculated CR decreased. This behaviour should be attributed to the corrosion products film formed on surface of the steel where it can limit the corrosion process. These results can explain the behaviour observed in the laboratory measurements and corroborates the formation of a corrosion products film, mainly iron sulphide, that it can be seen in the superficial analysis Table 3 shows the best fitting parameters of resistances obtained at turbulent flow conditions and, in the two test solutions. In this table it can be seen (in both test solution) that R_{ct} increased with time, consequently the corrosion rate decreased. Moreover, it is important to mention that the values of R_{ct} are smaller in turbulent flow than at static conditions. This fact should be attributed to wear of the corrosion products film by the action of the mechanical effects of the test solution movement. The results obtained by circuit equivalent analysis agree with the EIS graphic analysis and the LPR results.

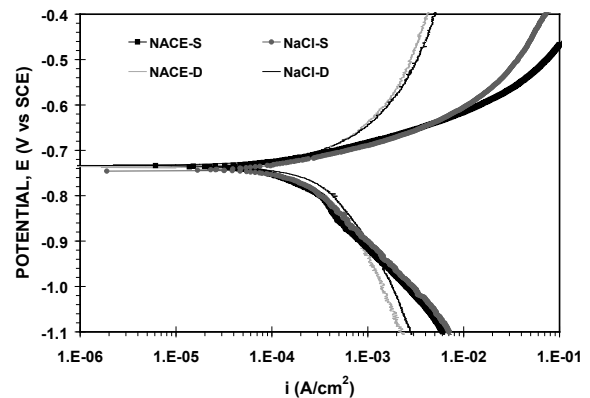


Fig. 8. Polarisation curves. X52 steel in NACE and 3.5% NaCl solutions saturated with H₂S at static (-S) and turbulent flow (-D) conditions and 60°C.

Table 3. Resistances obtained in the equivalent circuit analysis (Fig. 7b) corresponding to impedance spectra of the corrosion of the X52 pipeline steel immersed in 3.5% NaCl solution saturated with H₂S at static conditions and 60°C.

| Time (h) | R _s (Ω.cm ²) | R _{ct} (Ω.cm ²) | CR _{Ret} (mm/year) |
|----------------------------|-------------------------------------|--------------------------------------|-----------------------------|
| NACE Brine solution | | | |
| 0 (T0) | 17.6 | 69.18 | 4.36 |
| 4 (T4) | 29.48 | 78.50 | 3.84 |
| 8 (T8) | 44.21 | 80.17 | 3.76 |
| 12 (T12) | 64.89 | 80.60 | 3.74 |
| 24 (T24) | 17.61 | 82.32 | 3.66 |
| 3.5% NaCl Solution | | | |
| 0 (T0) | 6.05 | 62.53 | 4.82 |
| 4 (T4) | 8.99 | 87.38 | 3.45 |
| 8 (T8) | 12.36 | 95.70 | 3.15 |
| 12 (T12) | 13.99 | 108.6 | 2.78 |
| 24 (T24) | 19.09 | 120.6 | 2.50 |

Polarization Curves (PC)

In figure 8 is possible to see the polarization curves of the X52 pipeline steel in NACE and 3.5% NaCl solutions at turbulent flow and static conditions. Table 4 presents the relevant electrochemical parameter calculated from these polarisation curves. For the present work, the values of anodic and cathodic Tafel slope presented in this table were used in all calculations of CR. At both conditions, the calculated i_{corr} is higher in the 3.5% NaCl solution than in the NACE brine, consequently CR has the same behaviour. All calculated i_{corr} at turbulent flow conditions are higher than at static conditions. It is important to note that at turbulent flow conditions, the cathodic branches in these polarisation curves have slopes that cannot be associated to a pure charge transfer resistance process. This feature suggests a contribution of a mass transfer process on the cathodic kinetics. In addition, at this turbulent flow conditions, the anodic branches have slopes that it can suggest that a passivation process can influence the anodic reaction.

Table 4. Parameters obtained from the polarisation curves of the X52 pipeline steel immersed in NACE and 3.5% NaCl solutions saturated with H₂S at static and turbulent flow conditions and 60°C.

| Solution | b _a (v/decade) | b _c (v/decade) | E _{corr} (V vs SCE) | i _{corr} (A/cm ²) |
|--|---------------------------|---------------------------|------------------------------|--|
| NACE brine at static conditions | 0.0650 | 0.145 | -0.74 | 8.86x10 ⁻⁶ |
| 3.5% NaCl Solution at static conditions | 0.080 | 0.153 | -0.743 | 1.39x10 ⁻⁴ |
| NACE brine at dynamic conditions | 0.3100 | 0.3674 | -0.735 | 3.77x10 ⁻⁴ |
| 3.5% NaCl Solution at dynamic conditions | 0.2159 | 0.3308 | -0.735 | 4.03x10 ⁻⁴ |

In order to get the CR, a weight loss method was carried out. Table 5 shows the results of these tests. The behaviour of the results obtained by weight loss is agreed with the results of the electrochemical techniques (LPR, EIS and CP). At both conditions, the measured CR in 3.5% NaCl solution are higher than CR in NACE brine. In addition, all values of the CR at turbulent flow condition are higher than CR at static condition.

Table 5. Calculated CR by Weigh loss test of the X52 pipeline steel in NACE and 3.5% NaCl solutions saturated with H₂S at turbulent flow and static conditions and 60°C.

| Test solution | Weight loss (g) | CR (mm/year) |
|--|-----------------|--------------|
| NACE brine at static conditions | 0.0211 | 0.5328 |
| 3.5% NaCl Solution at static conditions | 0.0269 | 0.6777 |
| NACE brine at dynamic conditions | 0.0231 | 0.8577 |
| 3.5% NaCl Solution at dynamic conditions | 0.0462 | 1.7116 |

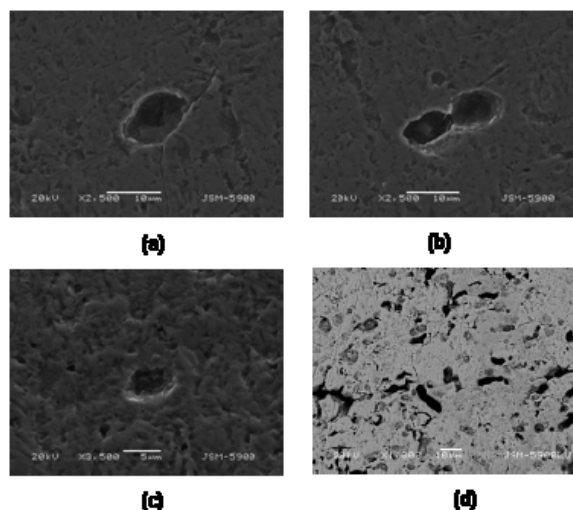


Fig. 9. SEM microphotographs of the X52 steel in NACE and 3.5% NaCl solutions at static (a and b respectively) and turbulent flow (c and d respectively) conditions at 60°C.

Surface analysis

Fig. 9 shows microphotographs obtained by SEM of the surface steel after experimentation was concluded. In these microphotographs is possible to observe that in both test solution and at static and turbulent flow conditions, a localized corrosion form was found. In addition, corrosion films formed on surface of the X52 pipeline steel was examined using X-ray diffraction. According to XRD diffraction results, in both solutions, mackinawite (Fe_{1-x}S), pyrrhotite (Fe_{1-x}S) and marcasite (FeS₂) were the iron phases found in corrosion products film. These results agree with some researchers²⁸⁻³⁰ about the steel corrosion in aqueous solution containing dissolved hydrogen sulphide.

CONCLUSIONS

According to the results of all techniques used in this research, the corrosion of X52 pipeline steel in 3.5% NaCl solution saturated with H₂S, is higher than in NACE brine solution saturated with H₂S.

In the two test environments (3.5% NaCl and NACE solution), at static and turbulent flow conditions, the calculated corrosion rate decreases with the increment of exposition time. This behaviour can be attributed to the formation of an iron sulphur film on the surface of the steel. In both environment and at turbulent flow condition, the increase and decrease of the CR can be attributed to broken and regeneration of the iron sulphur film. The film broken should be attributed to the mechanic effects, due to the movement of

the test solution on the corrosion film products formed on surface of the steel. It is important to note, that this effect reduce the iron sulphur film thickness formed on surface of the steel, consequently CR at turbulent flow condition is higher than at static condition.

There is not a clearly defined limiting current on the cathodic branch of the measured polarisation curves at turbulent flow condition; this fact suggests the presence of a flow independent process in the overall cathodic kinetics. On the other hand, at these conditions, the anodic branches showed that a passivation process should be influence in the overall anodic kinetic.

BIBLIOGRAPHY

1. L. M. Rodriguez-Valdez, et-al., *Corros. Sci.*, 48, (2006), 4053.
2. S. Arzola-Peralta, J. Mendoza-Flores, R. Duran-Romero and J. Genesca, *Corros. Eng. Sci. and Technol.*, 41, (2006), 321.
3. C. C. Silva, J. P. S.E. Machado, A. V.C. Sobral-Santiago, H. B. de Sant' Ana, J. P. Farias, *J. of Pet. Sci. and Eng.*, 59, (2007), 219.
4. C. Natividad, M. Salazar, R. Garcia, J. G. Gonzalez-Rodriguez, R. Perez, *Corros. Eng. Sci. and Technol.*, 41, (2006), 91.
5. F.D. de Moraes, F.L. Bastian, J. Ponciano, *Corros. Sci.*, 47, (2005), 1325.
6. R. Galvan-Martinez, R. Orozco-Cruz, J. Mendoza-Flores, A. Contreras, J. Genesca, "Hydrodynamics: Optimizing Methods and Tools", (Ed. H. E. Schulz, et-al), Chapter 16, INTECH OPEN ACCESS PUBLISHER, Croatia, (2011), 353-372
7. S. Arzola, J. Genesca, *J Solid State Electrochem.*, 9, (2005), 197.
8. P. H. Tewary, M. G. Bailey, A. B. Campbell, *Corros. Sci.*, 19, (1979), 573.
9. R. Galván-Martínez, J. Mendoza-Flores, R. Duran-Romero, J. Genesca-Llongueras, *Mat. and Corros.*, 55, (2004), 586.
10. G. T. Park, S. U. Koh, H.G. Jung, K.Y. Kim, *Corros. Sci.*, 50, (2008), 1865.
11. L.W. Tsay, Y.F. Hu, C. Chen, *Corros. Sci.*, 47, (2005), 965.
12. R. Galván-Martínez, J. Mendoza-Flores, R. Duran-Romero, J. Genesca-Llongueras, *AFINIDAD*, 62, (2005), 448.
13. B. Poulson, *J. Appl. Electrochem.*, 24, (1994), 1.
14. G. Kear, K. Bremhorst, Sh. Coles, Sh. H. Huáng, *Corros. Sci.*, 50, (2008), 1789.
15. G. Liu, D. A. Tree, M. S. High, *Corrosion*, 50, (1994), 584.
16. J.A. Wharton, R.C. Barik, G. Kear, R.J.K. Wood, K.R. Stokes, F.C. Walsh, *Corros. Sci.*, 47, (2005), 3336.
17. D. C. Silverman, *Corrosion*, 60, (2004), 1003.
18. R. Galvan-Martinez, R. Orozco-Cruz, R. Torres-Sánchez, *AFINIDAD*, 67, (2010), 442.
19. D. C. Silverman, *Corrosion*, 44, (2003), 207.
20. DR Gabe, et al., *J. of Appl. Electrochem.*, 28, (1998), 759.
21. G. Kear, B.D. Barker, K.R. Stokes, F.C. Walsh, *Corros. Sci.*, 47, (2005), 1694.
22. D. R. Gabe, DJ Robinson, *Electrochimica Acta*, 17, (1972), 1121.
23. R. Galvan-Martinez, R. Orozco-Cruz, R. Torres-Sánchez and E. A. Martínez, *Mat. and Corros.*, 61, (2010), 872.
24. J. L. Mora-Mendoza, J. G. Chacon-Nava, G. Zavala-Olivares, M. A. Gonzalez-Nuñez, S. Turgoose, *Corrosion*, 58, (2002), 608.
25. S. Papavinasam, R. W. Revie, M. Attard, A. Demoz, K. Michaelian, *Corrosion*, 59, (2003), 897.
26. K. Videm, J. Kvarekvål, *Mat. and Corros.*, 51, (1995), 260.
27. H. Vedage, T. A. Ramanarayanan, J. Mumford, S. Smith, *Corrosion*, 49, (1993), 114.
28. D. W. Shoesmith, P. Taylor, M. G. Bailey, D. G. Owen, *J. Electrochem. Soc.*, 127, (1980), 1007.
29. A. G. Wikjord, T. E. Rummery, F. E. Doer, D. G. Owen, *Corros. Sci.*, 20, (1980), 651.
30. B. G. Pound, M. H. Abdurrahman, M. P. Glicina, G. A. Wright, R. M. Sharp, *Aust. J. Chem.* 38, (1985), 1133.